Reaction Kinetics Mechanism for Chemiluminescent Species

Trupti Kathrotia, Uwe Riedel
Institute of Combustion Technology, German Aerospace Center (DLR) and University of Stuttgart
Stuttgart, Germany

1 Introduction

Luminescence occurring due to chemical excitation, referred to as $Chemiluminescence$, is found in the visible and ultra-violet (UV) band of the flame spectrum. In hydrocarbon flames the four major emitters found are OH*, CH*, C_2*, and CO_2* [1], here star (*) refers to electronically excited molecules. The spontaneous emissions of chemiluminescence species offer an inexpensive diagnostics of flames and combustion processes. It is non-intrusive in nature and allows to avoid expensive laser instrumentation. In early 1970s chemiluminescence has been identified as a marker for heat release, reaction zone and equivalence ratio, thereby providing a relatively easy diagnostics alternative for online measurement of these features in practical combustion applications. However, the relationship between chemiluminescence, heat release and equivalence ratio is relatively unknown except for a few correlations available in literature for a small range of conditions. The reaction kinetics mechanism that can explain the formation and consumption of these species is not well studied. Therefore it is of interest to develop a reaction mechanism which can predict the excited species measured at shock-tube and one-dimensional laminar flame experiments and that can be further used in combustion applications.

2 Chemiluminescence kinetics

The reaction kinetics of excited species is described by three reaction pathways. The formation reaction and their subsequent consumption by radiative decay and non-reactive collisional quenching reactions. The formation reaction of OH*, at about 306 nm in flame spectra, is suggested to be formed mainly by two possible reactions, the reaction of $CH + O_2 \rightarrow OH^* + CO$ and less known $CHO + O \rightarrow OH^* + CO$. In addition a three body reaction, $H + O + M \rightarrow OH^* + M$, playing an important role in hydrogen mixtures is suggested. The reaction rate of these three reactions, considered in current study are from Smith et al. [2], Haber et al. [3], Kathrotia et al. [4] respectively. CH* chemiluminescence is seen at 430 nm CH(A-X) and 390 nm CH(B-X) in flame spectra. About 80% of CH* seen in flames is from CH(A-X) transition whereas only 20% is from the other transition [2]. Three different reactions forming CH* are proposed in the literature,

$$C_2 + OH \rightarrow CO_2 + CH^*, \tag{1}$$

$$C_2H + O_2 \rightarrow CO_2 + CH^*, \tag{2}$$

Correspondence to: Trupti.Kathrotia@dlr.de

$$C_2H + O \rightarrow CO + CH^*. \tag{3}$$

However, it is unclear which reaction is important at a given condition. The rate of these reactions are taken from the recommendations of [2], [5], and [6] respectively. The chemiluminescence from the C_2(d-a) Swan band is mainly found between 470-550 nm in flame spectra. Few reactions are proposed for the formation of C_2* among which the reaction of CH_2 with C and C_2H with H was originally proposed by Gaydon (1974) [1]. The rate of these reactions are discussed in [6].

The formation of CH* and C_2* are linked to C_2, C_3 species via the reactions C_2 + OH → CO_2 + CH* and C_3 + O → CO + C_2^* respectively. Although these species are reactive in nature, a detailed study of these species is still unavailable. They are included in the present work due to their importance in CH* and C_2* formation chemistry. There is very few information available on the reactions forming and consuming these species and so they are not considered in most of the published reaction mechanisms so far. The measurement of the absolute C_2 concentration is difficult due to its low concentration (ppb levels) which requires more sensitive equipment. As shown in Figure 1 the chemistry of these species is closely linked to the C_2H_2 chemistry.

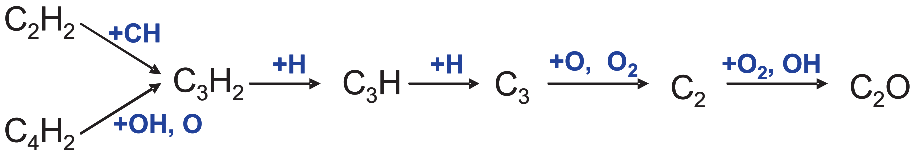

Figure 1: Reaction flow schematic of the C_2 formation pathway. The diagram shows how the C_2 formation is linked to the acetylene chemistry.

The dicarbon molecule C_2 can be found in its triplet $a(^3\Pi)$ and singlet $X(^1\Sigma_g^+)$ states. At flame temperatures, the triplet state, due to its higher degeneracy, is considered to be more populated (about 80%) [7]. Since few information is available on the formation and consumption reaction rates of these two states separately, we have considered the total C_2 from both states. Very recently few studies have discussed the C_2 measurement and its reactions in flames [7–9]. The main formation path of C_2 is through the reaction of C_3 with atomic and molecular oxygen. In addition the reaction of C_2H with O also leads to C_2. The important reactions consuming C_2 are with H_2, O_2, OH, O, CH, and CH_4. At very high temperatures (2500 - 3500 K) C_2O is formed from the above reactions.

3 Result and Discussion

The total kinetics model, including C_1 to C_4 hydrocarbons-, chemiluminescence- and C_2- reactions, consists of total 69 species and 924 reactions (forward and backward) [10]. The calculations of laminar one-dimensional flames are performed with the code INSFLA [11, 12]. Initial mixture composition, gas flow rate, temperature, and pressure at the burner surface are used as input.

The concentration of chemiluminating species is much lower compared to the concentration of ground state species. It is seen that their prediction depends on the species that are direct precursors responsible for their formation. These intermediates such as CH, C_2H, C_2, and $^1CH_2$ are not directly important for the global validation (such as ignition delay time, flame velocity) of the basic hydrocarbon oxidation mechanism. However, it is important to have a good prediction of such chemiluminescence precursor species. The underlying basic mechanism is originating from the dissertation of Heghes [13]. The C_1 to C_4 hydrocarbon mechanism is derived to model basic fuels at non-sooting conditions. The basic

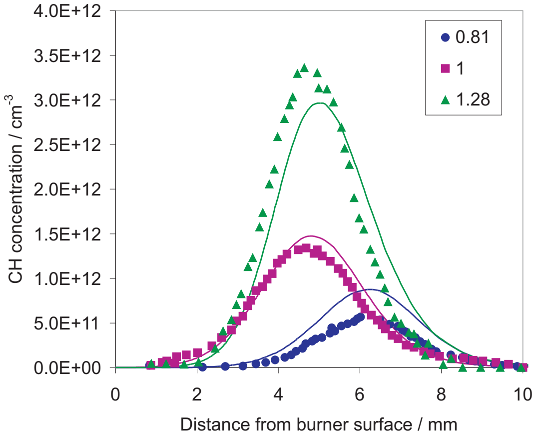

Figure 2: Comparison of measured and simulated absolute peak CH concentrations for lean (ϕ = 0.8), stoichiometric and rich (ϕ = 1.28) CH_4 - air flames. Symbols: experiments, Berg et al. [14]; Line: simulation.

mechanism which is extended to include the chemiluminescence mechanism was not optimized to accurately predict the chemiluminating precursors prediction. Therefore the mechanism is modified for the prediction of chemiluminescence precursor concentration.

Figure 2 presents prediction of CH concentrations measured by Berg et al. [14]. The simulated profiles at three different fuel stoichiometry are well predicted within the given error limit of ±15% (data precision) and ±35% (Rayleigh calibration) of the measurements. Only a few studies are dedicated to the measurement of absolute concentration of C_2 in flames due to its low concentrations which makes it difficult to measure [7–9]. In Figure 3, the comparison of measured and simulated C_2 concentrations are shown for the rich (ϕ = 1.28) methane-air flame. Many of the rate of the C_2 reactions are estimates from similar reactions or are available only at room temperatures. Extrapolation of room temperature rate to the flame temperature is not always applicable. Therefore, overprediction of factor of two is seen in the plotted simulated C_2. However, the peak position and the shape of the profile is well predicted.

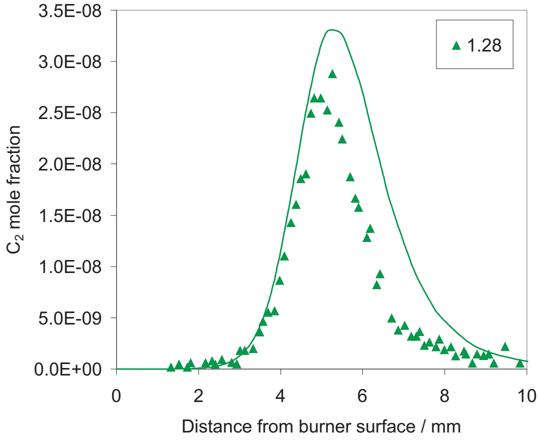

Figure 3: A comparison of measured and simulated C_2 concentrations in low pressure (0.04 bars) laminar premixed CH_4 - air flame (ϕ = 1.28) measured by Smith et al., [8]. Symbol: experiment; Line: simulation with the mechanism from the present work. Note that the simulated profile is divided by factor of 2.

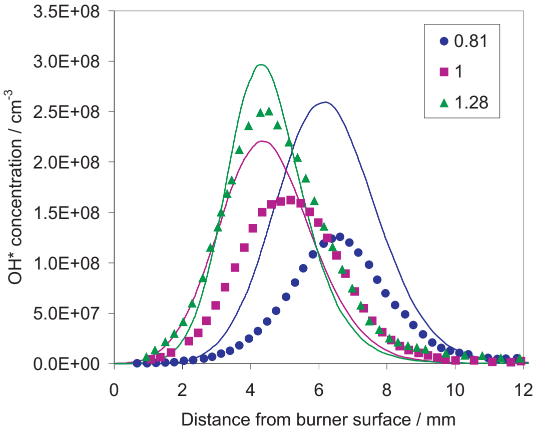

Figure 4: The OH* prediction of mechanism with the only OH* absolute concentration measured by Smith et al. [2] in methane-air premixed flames. The experiments are performed at lean, stoichiometric and rich flame condition (ϕ = 0.8, 1.0, 1.28) and the measured temperature profile is input to the simulation. Symbols: experiment, Line: simulation.

There are only few studies dedicated to the measurement of excited species. Among these are the premixed flame studies of Smith et al. [2, 6, 8] who measured all the three species (OH*, CH*, C_2*) in methane-air flames of varying stoichiometry.

Measurement of OH* is performed in series of methane-air lean (ϕ = 0.81), stoichiometric (ϕ = 1.0) and at rich flames (ϕ = 1.28) [2, 8]. In addition to the major path CH + O_2, the reaction CHO + O also has small contribution (30% lean-, 15% rich- CH_4 mixture) to the OH* formation. The shape and the peak position of OH* profile is well captured by the simulations. The OH* profiles are narrower and peak more closer to the burner surface when only CH + O_2 is forming OH*. However, the experimental trend of increase in OH* with increase in fuel stoichiometry is not reproduced at lean condition. At lean conditions the OH* absolute value is higher than at stoichiometric condition which is unclear to us as the prediction of OH* major precursor species CH is in agreement with the measurement.

The only CH* measurement done in laminar premixed flames are from Smith et al. [2]. They measured CH* at lean, stoichiometric and rich methane-air fuel conditions. The measured CH* intensity increases as the ϕ increases in the flame. The major species forming CH* is C_2H and as mentioned in [2] no mechanism can support the accuracy of it. Therefore, its uncertainty can be more than ±50%. This uncertaintly directly translates to the prediction of CH*. In addition to this there is a channel which forms CH* from C_2 . There are only a few mechanism which are capable of predicting C_2 concentrations [8, 9]. Therefore the accurate prediction of CH* is very challenging. When the reaction of C_2H + O_2 is considered in the mechanism, the CH* in lean flame is predicted very well with respect to the absolute concentration, peak position and shape of the profile. However, in stoichiometric and rich case it is under-predicted by factor of about 0.5. Therefore, in the later two cases, the other two reactions are also important. Taking only the C_2 + OH (1) reaction into account, results in CH* concentration underpredicted by factor of 3.5 to 6.5 when fuel composition is varied from lean to rich condition. And with this reaction included in the mechanism, the profile of the calculated CH* appears much later than measured CH* (lean condition) whereas in rich case it precedes the measurement. This explains that CH* at lean condition is formed earlier than C_2 and therefore reactions (3) and (2) are likely source of CH* in addition to the fact that C_2 concentrations are very low in lean mixtures. An analysis with these three reactions and their rate coefficients showed that better agreement with the measured absolute concentration, shape of profile and distance from burner is obtained when (3) is the only formation

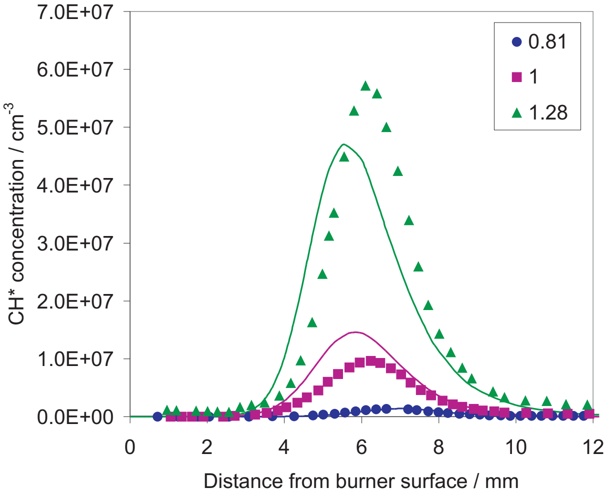

Figure 5: A burner stabilized premixed flame calculated with three different flame stoichiometries. The simulated CH* concentrations are compared with measurement [2] at low pressures (0.33 bars (ϕ = 0.8, 1.0), 0.04 bars (ϕ = 1.28)).

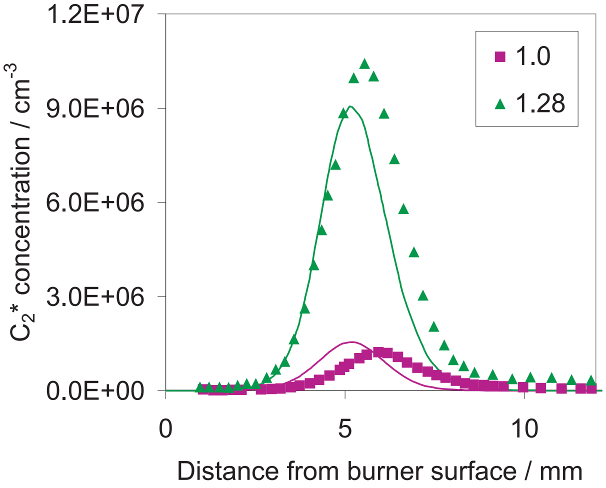

Figure 6: A comparison of C_2* absolute concentration measured by Smith et al. [2] with the simulations. The experiments are performed at stoichiometric and rich flame condition (ϕ = 1.28). Symbols: experiment, Line: simulation.

reaction in lean case whereas in stoichiometric and rich conditions both reactions (2) and (1) are included in the mechanism. The reported estimated measurement uncertainty to the CH* absolute concentration is about 35%.

The only measurement of C_2* for methane- air laminar premixed conditions have been done in [2] and later the same group studied stoichiometric and rich ethane- and ethylene- air flames [8]. The profiles of C_2* for the stoichiometric and rich methane-air flame, as shown in Figure 6, are in good agreement with the measurement. The shape of the rich profile matches very well with the measurement. However, in stoichiometric case it slightly precedes the measurement. With the recommended reactions and their rates in the mechanism, the absolute value of C_2* in both stoichiometric and rich cases are in agreement with the measurements.

4 Acknowledgement

The authors gratefully acknowledge the financial support from the Deutsche Forschungsgemeinschaft (German Research Foundation, DFG grant no. RI 839/4-2).

References

[1] Gaydon A. G. (1974). The spectroscopy of flames. Wiley: New York.

[2] Smith G., Luque J., Park C., Jeffries J., and Crosley D. (2002). Low pressure flame determinations of rate constants for OH(A) and CH(A) chemiluminescence. Combust. and Flame 131: 59.

[3] Haber L. C. and Vandsburger U. (2003). A global reaction model for OH* chemiluminescence applied to a laminar flat-flame burner. Combust. Sci. and Technol. 175: 1859.

[4] Kathrotia T., Fikri M., Bozkurt M., Hartmann M., Riedel U., and Schulz C. (2010). Study of the H+O+M reaction forming OH*: Kinetics of OH* chemiluminescence in hydrgen combustion systems. Combust. and Flame 157: 1261.

[5] Elsamra R., Vranckx S., and Carl S. (2005). CH(A) formation in hydrocarbon combustion: The temperature dependence of the rate constant of the reaction $C_2H + O_2 \rightarrow CH^* + CO_2$. J. Phys. Chem. A 109: 10287.

[6] Smith G., Park C., and Luque J. (2005). A note on chemiluminescence in low-pressure hydrogen and methane-nitrous oxide flames. Combust. and Flame 140: 385.

[7] Schofield K. and Steinberg M. (2007). CH and C_2 measurements imply a radical pool within a pool of acetylene flames. J. Phys. Chem. A 111: 2098.

[8] Smith G., Park C., Schneiderman J., and Luque J. (2005). C_2 Swan band laser-induced fluorescence and chemiluminescence in low-pressure hydrocarbon flames. Combust. and Flame 141: 66.

[9] Koehler M., Brockhinke A., Braun-Unkhoff M., and Kohse-Hoeinghaus K. (2010). Quantitative laser diagnostic and modeling study of C_2 and CH chemistry in combustion. J. Phys. Chem. A 114: 4719.

[10] Kathrotia T., Riedel U., and Warnatz J. (2009). A numerical study on the relation of OH*, CH*, C_2* chemiluminescence and heat release in premixed methane flame. Proceedings of the European Combustion Meeting Paper no. P809002.

[11] Maas U. and Warnatz J. (1988) Ignition processes in hydrogen-oxygen mixtures. Combust. and Flame 74: 53.

[12] Maas U. (1995) Coupling of chemical reaction with flow and molecular transport. Appl. Math. 40: 249.

[13] Heghes C. (2007). C_1 to C_4 hydrocarbon oxidation mechanism. PhD Thesis, Heidelberg.

[14] Berg P., Hill D., Noble A., Smith G., Jeffries J., and Crosley D. (2000) Absolute CH concentration measurements in low-pressure methane flames: Comparisons with model results Combust. and Flame. 121: 223.